1. Annual Report for 2005/2006

1. Zwischenbericht für den Zeitraum 2005/2006

DFG Research Group FOR575

High Frequency Parasitic Effects in Inverter-fed Electric Drives

Höherfrequente Parasitäreffekte in umrichtergespeisten elektrischen Antrieben

Prof. Dr.-Ing. habil. Andreas Binder (Sprecher)
Prof. Dr.-Ir. Herbert De Gersem
Prof. Dr.-Ing. Volker Hinrichsen
Prof. Dr.-Ing. Peter Mutschler
Prof. Dr.-Ing. Thomas Weiland

Darmstadt, February 2007

Responsible for the report:

Prof. Dr.-Ing. habil. Andreas Binder, geb. 16.7.1957
Technische Universität Darmstadt
Institut für Elektrische Energiewandlung
Fachbereich 18 - Elektrotechnik und Informationstechnik
Landgraf-Georg-Straße 4, D-64283 Darmstadt
Telefon: 06151/16-2167, Fax: 06151/16-6033
E-Mail: abinder@ew.tu-darmstadt.de

1. Summary

This report summarizes the results of the 1st phase of the research work of the DFG Forschergruppe FOR575. A presentation of the research members and a short overview on the done work during the first year of research is given.

2. Motivation

The DFG Research Group FOR575 "High Frequency Parasitic Effects in Inverter-fed Electric Drives" (Höherfrequente Parasitäreffekte in umrichtergespeisten elektrischen Antrieben) was installed at TU Darmstadt in late 2005. A first intermediate report shall document the achieved results so far.

3. Introduction and Overview

The DFG Research Group FOR575 started with its work in October 2005 with the first 2 projects. The finding for well-suited researchers for the other topics took until mid-August 2006. By that time the staff of the group became complete. Therefore the results of the different projects are on different stages. Project No. 4 was not granted by DFG, but was meanwhile financed by industry (Johannes Hübner GmbH, Giessen), so it joined the group by this way. Project No.6 was also not granted, so it was skipped. Hence the originally listed project no.7 was renamed as new no.6 in this report.

TP1-Binder	Berechnung parasitärer hochfrequenter Stromverteilungen in elektrischen Maschinen bei Umrichterspeisung;
TP2-Binder	Vergleichende Untersuchung von Verlusten in umrichtergespeisten Maschinen durch höherfrequente Stromanteile mit Zeitschrittverfahren;
TP3-DeGersem	Simulation von Wellenausbreitungsphänomenen in umrichtergespeisten Antrieben;
TP4-Hinrichsen	Dimensionierung, Alterungsverhalten und Energieaufnahmevermögen von Metalloxid-Varistoren zum Überspannungsschutz von umrichtergespeisten Antrieben;
TP5-Mutschler	Wechselwirkung zwischen Schaltverhalten und Steuerung der Leistungstransistoren mit HF-Strömen und Spannungen in Antrieben am Spannungszwischenkreis Wechselrichter;
TP6-Mutschler *Skipped*	Höherfrequente Parasitäreffekte in Antrieben mit unkonventionellen Umrichtern;
TP7-Weiland *Renamed no.6*	Multiskalenmodellierung und Parameterextraktion in der Simulation umrichtergespeister Antriebe.

Overview on the research topics:

The first topic is concerned with high frequency parasitic currents in electrical machines, whose main cause is common-mode voltage. These currents can represent great danger for the bearings. Creating and researching high frequency equivalent circuit is inevitable part of this subproject.

The topic 2 is related to additional losses in electrical machines, induced by high order time harmonics of current in inverter-fed drives. They are especially noticeable as eddy current losses in iron and, in the case of synchronous permanent magnet machines, in permanent magnets.

The aim of the third subproject is to build a model of the whole drive system, consisted of inverter, cable and motor. Special attention will be paid to the case of long cable. This subproject is based entirely on simulations, and it should research in detail possible over-voltages.

The focus point of the fourth subproject is application of ZnO varistors for over-voltage protection of inverter-fed electrical drives. The key issue here is to find the way for proper dimensioning of ZnO varistors. Also the question of varistor ageing is very important here.

The fifth project belongs to scientific area of power electronics. An inverter with possibility of collector current measurement was built for experiments. The aim is to optimize the control algorithm of transistors, so that over-voltages and common-mode voltage become as small as possible.

With the subproject 6 it is intended to compute thermal behaviour of ZnO varistors and the risk of electric breakdown in bearings due to capacitive high-frequent currents. The approach used is Finite Integration Technique (FIT).

The researcher group is internationally organized with 6 researchers (5 of them are PhD students, one is a post-doc) from Germany, Romania, Serbia, Turkey. Hence working language and all reports are given in English. The group is meeting on regular intervals each 8 … 10 weeks together with their tutoring professors to report on their work via PowerPoint presentation. Actual presentations and all meeting protocols are available at the FOR575 homepage:
http://www.ew.e-technik.tu-darmstadt.de/for575/DEUTSCH/index.html
http://www.ew.e-technik.tu-darmstadt.de/for575/ENGLISH/
Dr. De Gersem held in Summer half term 2006 a special lecture „FEM Machine Simulation“ for the members of FOR575 and for interested students with 2.0 hours per week. The ppt transparencies of the lectures are available at the above noted home page.
A workshop of the researchers was performed at TU Darmstadt on January 18th 2007, where the researchers gave closer information on their work done so far, looking for closer co-operation concerning the exchange of software, measurement results and theoretical models. The members of the group are presented on the home page and are shortly presented in the following.

4. Research members of FOR575

The members are listed according to the projects:

Subproject 1: Calculation of parasitic high frequency current distribution in inverter-fed electrical machines

Dipl.-Ing. Oliver Magdun (Romania), Tutor: Prof. A. Binder

Subproject 2: Comparative analysis of losses in inverter-fed machines caused by high frequency current components using time-stepping

Dipl.-Ing. Ljubisa Petrovic (Serbia), Tutor: Prof. A. Binder

Subproject 3: Simulation of wave propagation phenomena in inverter-fed drives

Dr.-Ing. Dipl.-Phys. Olaf Henze (Germany), Tutor: Prof. De Gersem

Subproject 4: Ageing mechanisms and energy handling capability of metal-oxide varistors for overvoltage protection in inverter-fed drives

Dipl.-Ing. Alexander Rocks (Germany), Tutor: Prof. Hinrichsen

Subproject 5: Influencing the voltage slope at the inverter output by modifying the switching behaviour of the IGBT power modules, accomplished by special gate drivers

Dipl.-Ing. Calin Purcarea (Romania), Tutor: Prof. Mutschler

Subproject 6: Multiscale modelling and extraction of parameters in the simulation of inverter-fed drives

M.Sc. Zarife Cay (Turkey), Tutor: Prof. Weiland

5. Subproject 1: Calculation of Parasitic High Frequency Current Distribution in Inverter-Fed Electrical Machines

Prof. Dr.-Ing. habil. Andreas Binder
Dipl.-Ing. Oliver Magdun
Institut für Elektrische Energiewandlung, TU Darmstadt
E-Mail: omagdun@ew.tu-darmstadt.de

5.1 Orientation, Classification of HF - current distribution and definition of sub-problems

The major cause of parasitic high frequency currents in inverter-fed electrical machines have been found to be the common – mode voltage with high frequency and high dv/dt [5.1], [5.2], [5.3], [5.4]. When the three-phase induction motors are fed by high frequency inverters, the distribution of the common mode voltage between parasitic capacitances from the motor (see Fig.5.1) will cause a capacitive shaft voltage and a path for a high frequency common-mode current [5.1]. Due to big value of stator winding – stator core capacitance C_{WS}, the most important part from common mode current will flow through C_{WS} to ground and other part due to capacitance C_{WR} is to choose the bearings path [5.5].

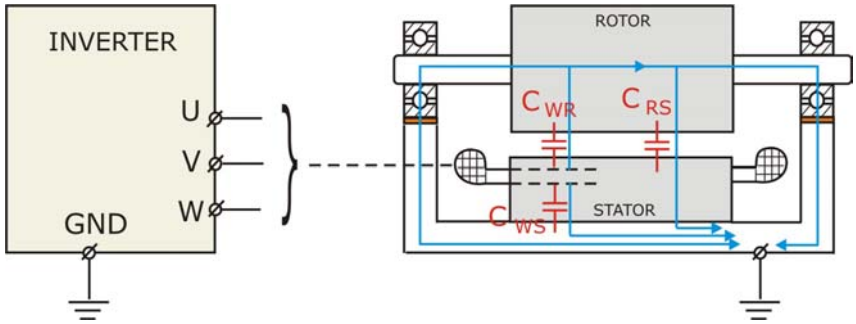

Fig. 5.1. Stray capacitances of the induction motor

The high frequency common-mode current will generate a circumferential magnetic flux in the stator core, which causes an induced shaft voltage. The two types of high-frequency shaft voltages, capacitive shaft voltage and induced shaft voltage, are the reason for high-frequency circulating bearing currents and discharge bearing currents, respectively. Hence, in inverter-fed electrical machines four types of parasitic high frequency currents can be founded: common mode currents, high frequency circulating bearing currents, electrostatic discharge currents (EDM –

currents) due to lubrication film discharging between balls and running surface and capacitive bearing currents (very small and nondestructive for motors).

5.2 Computation of common mode currents

To compute these currents, in literature several models have been proposed. For computation of **common mode current** two models are more known: a simplified circuit model [5.3], [5.5] and a detailed model [5.6], [5.7]. For this report only the simplified model has been checked. The stray capacitances of this model have been computed analytical with formulas conform [5.4], [5.5], [5.8] and numerical and the difference between the results has been explained.

Results obtained for motors with three levels of power: 11 kW, 110 kW and 500 kW show a good concordance between analytic results and numeric results for C_{WS} and C_{SR}, and a big difference between analytic results and numeric results for winding stator - rotor capacitance C_{WR}. The importance of C_{WR} can be seen very easy analysing the bearing voltage ratio BVR [5.2]:

$$BVR = \frac{C_{WR}}{C_{WR} + C_{SR} + 2 \cdot C_B} \tag{5.1}$$

Because of C_{WR} and bearing capacitance $C_B \cong C_{B1} \cong C_{B2}$ are approximately 20 times smaller then C_{SR} [5.5], one can conclude that the BVR is direct proportionally with C_{WR}. An error in computation of C_{WR} means an error in computation of BVR and due to the shaft voltage is:

$$v_R = BVR \cdot v_{CM}, \quad (v_{CM} \text{ is common mode voltage}) \tag{5.2}$$

An error in shaft voltage computation is to result. Hence, the design of the induction motor to reduce the shaft voltage is affected by errors if only analytical formulas from literature are used. Because of, in generally, designing of electrical machines is done with analytical formulas before of a numeric computation, in this report, two correction factors for analytical formula from literature have been proposed. They show the fact that for computation of C_{WR}, not all the length of the stator slot opening has to be considered, but only an equivalent length of this. These factors of correction should be used in analytical formulas of winding stator - rotor capacitance to get the best results.

In order to compute the circuit capacitances with numerical methods faster, the field problem has been reduced to a single slot. Using ANSYS software, the field problem has been electro-statically solved and the capacitances have been computed, processing the field problem solution using two methods: electric field energy and Maxwell's equations. It has been founded that the second method is faster than the first method, but in general this thing depends on the capability of the software used to offer the results and processing them.

Computation of common mode current has been done with two methods: the first, with the classical model using the stray capacitances computed with electrostatic methods and the second: an original method with a transient solving of a hybrid model: circuit-FEM 2D. Since the hybrid model is derived from the classical model, the results obtained are the same for the two methods and the computation of stray capacitances with electrostatic methods is checked. When the computed results have been compared with measured results of common mode ground current, differences has been observed. After checking on many motors, it has been concluded that stator iron influence should be considered in different way.

The computation of **EDM – currents** could be done by two methods: the first, with bearing voltage imposed and using a simplified circuit [5.4] and the second, using the classical model with a special loop for currents computation, method which was analysed for this report. The advantage of the analysed method is the fact that it gives the computed results near the experimental results, but to apply this method all parameters of equivalent circuit are required. In comparison with the second method, the first method has the advantage that the resistance and

inductance of the common ground current path are not required for computation, but it has a big disadvantage because of the bearing voltage at break down must be known as an entry data for the simplified model, but it needs special equipment to measure it [5.4]. Hence, analysing the problems regarding to the calculation of parameters of classical equivalent circuit, one can conclude that the method exposed in [5.4] remains at this moment the first alternative in EDM-currents computation.

An equivalent circuit for the calculation of **high frequency circulating bearing** has been proposed in [5.9]. This model uses the common mode current as an input source and the problem with the computation of common mode current has been already exposed. However, a good solution from the common mode current computation will give a good solution for all parasitic high frequency currents computation.

With only 5-10 mA amplitude [5.4], **capacitive bearing currents** are not harmful for induction motors. A model to compute capacitive bearing currents has been proved to not be necessary.

5.3 Aspects regarding to the software used

In order to compute parameters of equivalent electrical circuits proposed in literature numerically, ANSYS software has been used and to solve the equivalent circuits for high frequency currents, both SPICE and ANSYS have been used.

Using two different programs to solve electrical circuits a comparison between them was been possible. SPICE is a dedicated program to solve electrical circuits and the solving time from the start to the end of the problem, with all stages: pre-processing, solving and post-processing is incomparably shorter than the solving time of ANSYS. ANSYS keeps the same rules for problem pre-processing in all cases: finite element solving or electric circuits solving. For example, a simple circuit with three elements and a source of voltage needs at least 20-25 lines of program plus the geometrical coordinates of the elements. On the other side, the electrical circuit must be designed exactly in the order in which the current is to flow through the circuit. These are some problems for ANSYS, but ANSYS is a dedicate program to solve the finite element problems and not electrical circuit problems.

5.4 References

[5.1] S. Chen, T. Lipo, D. Fitzgerald, „Source of Induction Motor Bearing Currents caused by PWM inverters“, IEEE Transaction on Energy Conversion, vol. 11, no.1, pp.25-32, March 1996

[5.2] D.Busse, J. Erdman, R. Kerkman, D. Schlegel and G. Skibinski, “Characteristics of Shaft Voltage and Bearing Currents”, IEEE Industry Applications Magazine, November/December, 1997

[5.3] F. Fereira, P. Pereirinha, A. Almeida, „Study on the bearing Currents Activity in Cage induction Motors using Finite Element Method“, Proceedings of the 16th International Conference on Electrical Machines (ICEM 2004), Athens, Greece, 2006

[5.4] A. Mütze, „Bearing Currents in Inverter-Fed AC-Motors“ Shaker Verlag, Aachen 2004

[5.5] D. Busse, J. Erdman, R.Kerkman, D.Sclegel, G. Skibinski, System Electrical Parameters and their Effects on Bearing Currents, IEEE Transaction on Industry Application, vol.33, no.2, Mar./Apr.1996

[5.6] S. Chen, T. Lipo, D. Fitzgerald, „Modeling of Motor Bearing Currents in PWM Inverter Drives“ , IEEE IAS Annual Conference Records, 1995, Vol.1

[5.7] P. Mäki-Ontto, J. Luomi, „Induction Motor Model for the Analysis of Capacitive and Induced Shaft Voltages“ , 0-7803-8987-5/05, IEEE

[5.8] P. Maeki-Ontto, J. Luomi, „Design of Converter-Fed Induction Motors to Reduce Bearing Currents“, Proceedings of the 16th International Conference on Electrical Machines (ICEM 2004), Cracow, Poland, 2004

[5.9] A. Mütze, A.Binder,”Calculation of Circulating Bearing Currents in Machines of Inverter-Based Drive Systems”, in Proc.39th IEEE IAS Annu.Conf., Seattle, WA, 2004, vol.2, pp.720-726

6. Subproject 2: Comparative analysis of losses in inverter-fed machines caused by high frequency current components using time-stepping

Prof. Dr.-Ing. habil. Andreas Binder
Dipl.-Ing. Ljubisa Petrovic
Institut für Elektrische Energiewandlung, TU Darmstadt
E-Mail: lpetrovic@ew.tu-darmstadt.de

6.1 Modelling of permanent magnet machines in 2D

The work has begun at December 15th, 2005. In the first month theoretical introduction to Finite Element Method (FEM), as well as to higher order harmonic phenomena in electrical machines, was given. After that the researcher made his first steps in FEM practice, learning the basics of the program FEMAG. As this program does not have time-step capabilities which are necessary for the project, it was used just for a first experience with FEM programs.

The first big decision in the project was to determine for which parts of the subproject ANSYS, at the Institute for Electrical Energy Conversion already existing FEM software, should be used. Because of the good previous experiences with ANSYS solving thermal 3D computations, it was right from the beginning clear that ANSYS will be used for that. It is able to do 2D and 3D multiphysics computations, so it could have been appropriate for the whole subproject. The use of only one program for the whole subproject would be by all means advantageous. However, there was no any experience in ANSYS concerning the magnetoquasistatic transient (i.e. time-stepping) computations with circuit coupling, which represent the core of the subproject. At a first glance, it appeared realistic that ANSYS can do the job because all components needed were there. The simulations where started on a model of coil with magnetic circuit. The idea was to get insight into the technique using this model with small number of elements, and then to change to motor in a week. The magnetic circuit was considered in two variations: with and without air gap. The model of PWM inverter to supply the winding was developed from scratch in ANSYS's programming language called APDL. After the four months of work the following conclusions emerged:

- magnetic flux and losses calculations gave correct results
- not only the winding, but also the eddy current regions have to be defined as conductors connected to the circuit
- there is a constraint in ANSYS that conductors attached to a circuit cannot move
- it follows from the previous two points that ANSYS cannot compute the simulation of electrical motor, as it, unlike the coil, has moving parts.

Therefore another FEM program, FLUX2D, had to be acquired. FLUX2D has additional advantages: iron losses as special post-processing option and faster solver. It should be noted that both programs were used on the edge of their capabilities, because considering of high frequency parasitic effects in FEM is computationally intensive and represent new research area. Hence, the FEM software doesn't have related experience. This means that even FLUX2D support was not always able to give the right advice, that sometimes various bugs (e.g. losses were once in ANSYS less than 0) and other technical difficulties occurred.

The change to FLUX2D meant that another initial training was needed, in order to learn how to use it. The simulations were right from the beginning done on the model of permanent magnet synchronous machine (PMSM). The PMSM machine with buried magnets I-C, developed in our laboratory, was picked as the object of simulations (Fig. 6.1).

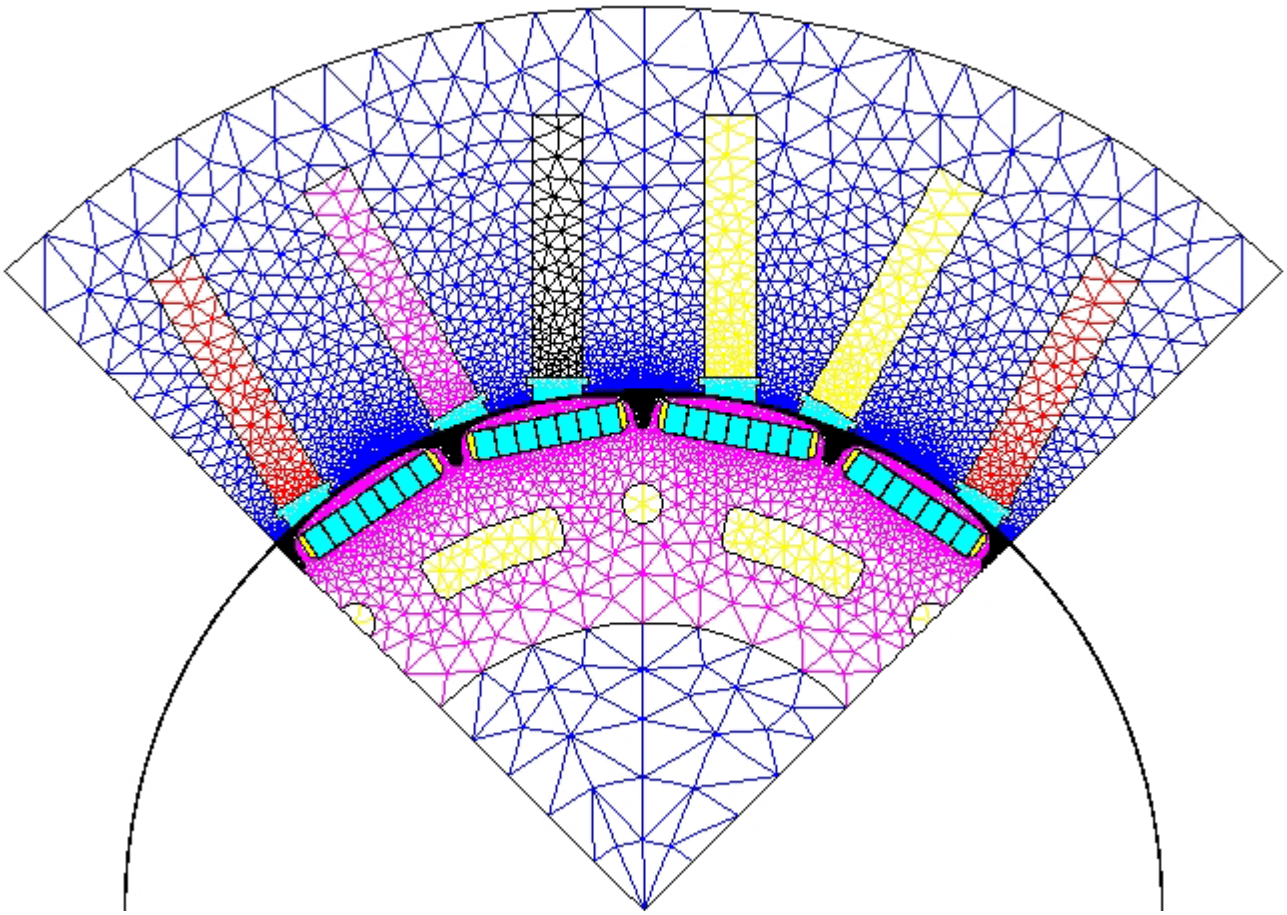

Fig. 6.1: Meshed geometry of the prototype permanent magnet motor type I-C, modeled with FLUX 2D

6.2 Calculation results for eddy current losses within permanent magnets in 2D

P_m [W]	n=1000 /min	n=3000 /min
Cascading method		
no-load	0.42	3.8
load	36	89
time-step method		
no-load	0.19	1.7
Load	24	57
modified cascading method		
no-load	0.27	2.4
Load	23	56

Table 6.1: Calculated eddy current losses in all permanent magnets of buried PMSM, calculated with FLUX2D

The same machine was previously simulated with FEMAG. The corresponding measurement results are already existing, so there is no need to wait the end of the project in order to be able to compare simulations results with measurements. The results of FLUX2D showed good agreement with measurements (e.g. no-load voltage). Of course, FEMAG doesn't have all the capabilities of FLUX2D. The results calculated directly by FEMAG showed very good agreement with FLUX2D. However, in FEMAG eddy-current losses in permanent magnets had to be calculated in indirect way, by "cascading" method, unlike FLUX2D. The cascading method consists of one

static DC and one steady state AC calculation (Table 6.1). The first results for losses by cascading method were presented in [6.1]. The time-stepping computations with FLUX2D showed that those values were too high. The insight obtained by more general time-stepping method enabled the modification of the cascading method, so the much more accurate results could come up. Modification means that instead of one area for flux recording in the first cascade three are used (Fig. 6.2). It is worth noting that the results are in agreement with expectations based on [6.2] and [6.3]. It is worth mentioning that rated speed of the machine is n = 1000/min, while n = 3000/min is maximum speed, yielded by flux weakening in the load case. The simulation was done using injecting of sinusoidal stator current.

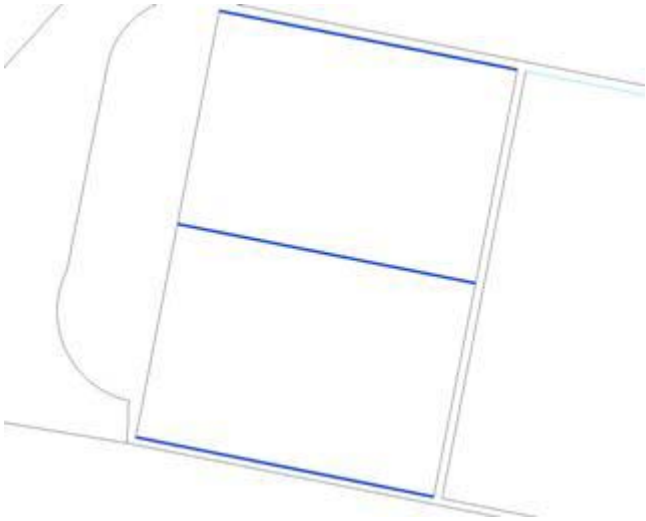

Fig. 6.2. Modification of loss calculation in a buried magnet using the flux variation within three layers on the upper and lower edge and in the middle

After PMSM with buried magnets were investigated, the same procedure was applied to a PMSM with surface mounted magnets. The motor was built by industry. This time, however, the simulations were extended to account for eddy current iron losses in rotor. When rotor is laminated their amount is negligible, but not in the case with massive iron, which also have considerable importance in practice [6.4], [6.5]. Another extension were considering of massive magnets instead of segmented (Table 6.2).

P_m[W] / $P_{Fe,Ft}$ [W]	f=2500 Hz, I_{peak}=1.7 A	f=5000 Hz, I_{peak}=1.3 A	magnets	rotor iron yoke
case 1	16/ 0.12	15/ 0.1	segmented	laminated
case 2	56/ 0.12	58/ 0.1	massive	laminated
case 3	52/15	54/15	massive	massive

Table 6.2: Calculated eddy current losses in all permanent magnets and rotor iron yoke of a PMSM with surface mounted magnets

Also an analytical formula for calculation of time harmonic losses, described in [6.5], was applied to the surface mounted machine. It gave 12% greater results, which is satisfactory. This formula has limitation that it doesn't account for higher order spatial harmonics and therefore it would be interesting to use it for one more time with more appropriate machine.

It is also possible to use cascading method with analytical formula as second cascade, instead of steady state AC computation. This alternative is often simpler for practical use. Also here

comparison with the time-stepping solution appeared to be useful. The flux through the upper edge of a magnet represents connection between the two subsequent cascades. When an analytical formula is used, the area which the flux flows through should not be the same as in the original method (Table 6.3). In this way the discrepancy between cascade with formula and original cascade becomes totally negligible, as it should be. It declines in this specially created example from 10% to 0.0003%.

$P_{m1,1}$ [W]	old area	new area
original cascading	0.01851	0.020820
cascading + formula	0.02055	0.020814

Table 6.3: Calculated eddy current losses in one magnet segment for one flux time harmonic

The simulation with inverter-feeding of the stator was done for the case of the machine I-C with buried magnets, rotation speed 1000 rpm, at rated load. Eddy current losses in magnets were 33 W, which is clearly (about 30%) more than 25.5 W for sinusoidal current. The same conclusion were given in a similar consideration in [6]. As a result of this simulation, also current waveform with its ripple was obtained. The current waveform was also yielded by measurements. For the spectrum of the stator current there is simple prediction of pronounced frequencies, very well known from the theory. This third way is the most reliable one. The current spectrum from FLUX2D corresponds to the theoretical spectrum much better than the measurement. This is so because harmonics near the switching frequency appeared not to be enough pronounced in the measurement results.

6.3 References

[6.1] C. Deak, A. Binder, K. Magyari: “Magnet Loss Analysis of Permanent-Magnet Synchronous Motors with Concentrated Windings”, ICEM 2006, September 2006, Chania, Greece, 6 pages
[6.2] M. Nakano, H. Kometani, M. Kawamura: “A Study on Eddy-Current Losses in Rotors of Surface Permanent-Magnet Synchronous Machines”, IEEE Transactions on Industry Applications, vol.42, No.2, March/April 2006
[6.3] H. Polinder: “On the losses in a high-speed permanent-magnet generator with rectifier - with special attention to the effect of a damper cylinder”, PhD thesis, Delft University of Technology, Netherlands 1998
[6.4] T. Lu: “Weiterentwicklung von hochtourigen permanenterregten Drehstromantrieben mit Hilfe von Finite-Elemente-Berechungen und experimentelle Untersuchungen”, PhD thesis at TU Darmstadt, Shaker Verlag, Aachen 2004
[6.5] A. Binder: “Analytical calculation of eddy current losses in massive rotor parts of high speed permanent magnet machines”, SPEEDAM Proceedings, June 2000, Ischia, Italy, p. C2-1/C2-6
[6.6] D. Ishak, Z.Q.Zhu, D. Howe: “Eddy-Current Loss in the Rotor Magnets of Permanent-Magnet Brushless Machines Having a Fractional Number of Slots Per Pole”, IEEE Transactions on Magnetics, vol.41 (2005), No.9

7. Subproject 3: Simulation of wave propagation phenomena in inverter-fed drives

Dr. Olaf Henze
Prof. Dr.-Ir. Herbert De Gersem
Institut für Theorie Elektromagnetischer Felder, TU Darmstadt
E-Mail: henze@temf.tu-darmstadt.de

Meanwhile Prof. De Gersem moved to the Catholic University of Leuven, Belgium, but can manage to be regularly in TU Darmstadt to supervise Dr. Henze.

7.1 Introduction

Aim of the first three months of the project was to find a network model which describes the system inverter-cable-motor as a whole. This model should be the basis of deeper research of the different parts of the system later. Our goal is to determine the steady-state behaviour of the cable and the motor. This will result in a model which allows calculating the voltage at the motor side in the frequency domain. The voltage at the motor terminals caused by a general periodic signal like an inverter signal can then be calculated by using Fast Fourier Transformation.

7.2 Network-Model

a) Cable

The cable is modelled by the approach presented in [7.1]. It is important, that in our case a three-phase cable is needed to connect the inverter with the motor. Hence a General Transmission Line Model of the cable is needed, in which the coupling of the inductors and the capacitors between the three phases of the cable is considered. A decoupling of the 3 phases can be reached by finding the Eigenvectors and –values of the coupling matrix. This results in three different modes: the common-mode (0-mode), and two differential modes (1-mode, 2-mode). It is significant that the propagation constant and the wave impedance of the common mode are different from the constants of the differential modes.
The decoupling of the three phases in the three modes makes it possible to apply the common transmission line theory to the three modes. That results in three transfer functions, which connect the three input voltages with the three voltages at the induction motor.

b) Induction-Motor

The model of the induction motor is based on the (abc)-approach [7.2]. In the stationary case the system of six differential equations can be reduced to a linear algebraic system which connects the stator voltages with the stator currents. The obtained matrix is an impedance matrix. Also in this case, a transformation in the (012)-system results in a decoupling of the currents and the voltages. The new impedances can be identified as the impedances which are arising in the three transfer functions which describe the behaviour of the three-phase cable.

c) Inverter

To create the inverter signal a triangle pulse is compared with a sinusoidal signal. This procedure is the basis of the Pulse-Wide-Modulation (PWM). If the sinusoidal pulse is bigger then the triangular pulse, the voltage of the inverter is set to +U; in the other case the voltage is –U. The resulting signal is a sequence of rectangular pulses with different pulse lengths. After interaction with the cable-motor system operating as a low-band filter, the pulse train more or less decays to the sinusoidal signal. To calculate the voltages at the motor side it is necessary to transform the inverter signal into the frequency-domain. This can be performed by Fast-Fourier-Transformation. After transformation into the (012)-system, multiplication with the transfer-functions and back transformation into the (abc)-system, the voltages at the induction motor can be obtained.

d) Example

To test the model the behaviour of the voltages at the motor is examined with parameters chosen from [7.2], [7.3] and [7.4]. In this example two different cable lengths are used. The time step related to the sampling rate of the discrete Fourier Transformation is chosen to 50 nm. The results

are shown in Fig. 7.1 and 7.2. It is obvious that over a certain cable length between 5 and 50 meters overvoltages arise which are three times as big as the impressed voltage in this case.

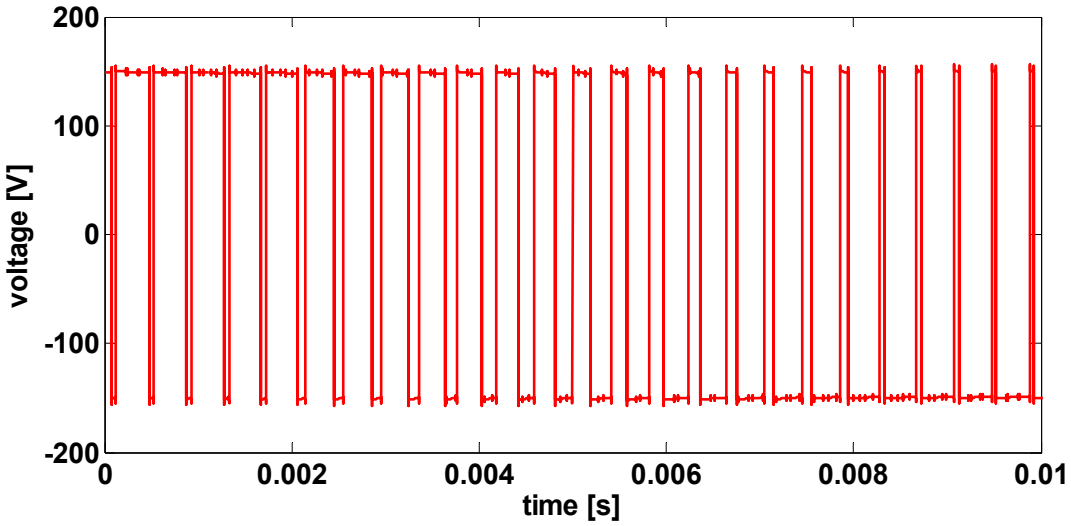

Fig.7.1: Calculated phase voltage at the induction motor with a cable length of 5 m

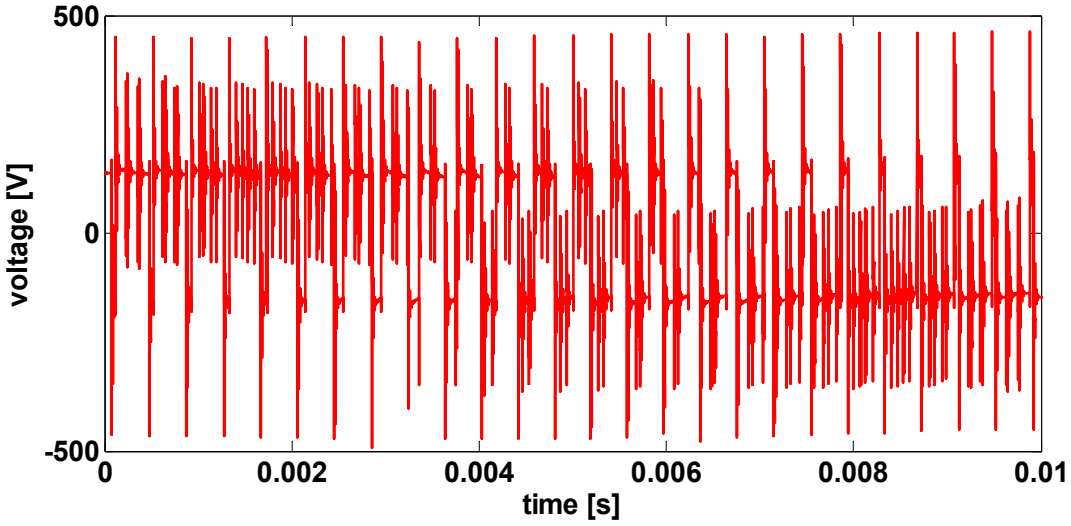

Fig. 7.2: Calculated phase voltage at the induction motor with a cable length of 50 m

7.3 Problems and Outlook

It is obvious that the network model gives only a rough description of the behaviour of the whole system. In the cable thermal effects are not considered. In the network-model of the induction motor capacitive effects, which should arise in the high frequency domain, are missing completely. Hence in a next step field examinations are necessary to get insight into the behaviour of the parasitic effects in the cable and motor. This will be performed via Finite-Integration and Finite-Element Techniques.

7.4 References

[7.1] Bolsens, De Brabandere et al., "Transmission Line Effects on Motor Feed Cables: Terminator Design and Analysis in the Laplace Domain", International Electric Machines and Drives Conference (IEMDC), (CD-Rom), Madison, Wisconsin, USA, June 1-4, 2003

[7.2] Pillay, Lewis,"Mathematical Models for Induction Machines", IEEE, IAS Annual Meeting October 1995, pp.606-616
[7.3] Skibinski, Kerkman et al.,"Reflected Wave Modelling Techniques for PWM AC Motor Drives" IEEE Applied Power Electronics Conference Anaheim, CA, February 15-19, 1998, pp. 1021 - 1029
[7.4] Mutschler, "Grundlagen der Energietechnik", Vorlesungsskript SS1996

8. Subproject 4: Ageing mechanisms and energy handling capability of metal-oxide varistors for over-voltage protection in inverter-fed drives

Prof. Dr.-Ing. Volker Hinrichsen
Dipl.-Ing. Alexander Rocks
Fachgebiet Hochspannungstechnik, Institut für Elektrische Energiesysteme, TU Darmstadt
E-Mail: rocks@hst.tu-darmstadt.de

8.1 Introduction

The described subproject deals with the protection of the machine winding of inverter-fed drives against over-voltages caused by traveling waves on electrically long lines. Under supposition of almost ideal reflection factors at the machine and at the inverter

$$r_{U,\text{machine}} <\approx 1 \tag{8.1}$$

$$r_{U,\text{inverter}} >\approx -1 \tag{8.2}$$

the voltage at the end of the line gets reduplicated compared to the intermediate-circuit voltage when the inverter and the drive are connected to each other by an electrically long line. At an impulse rise time of 100 ns "electrically long" means a length of 7,50 m and longer.

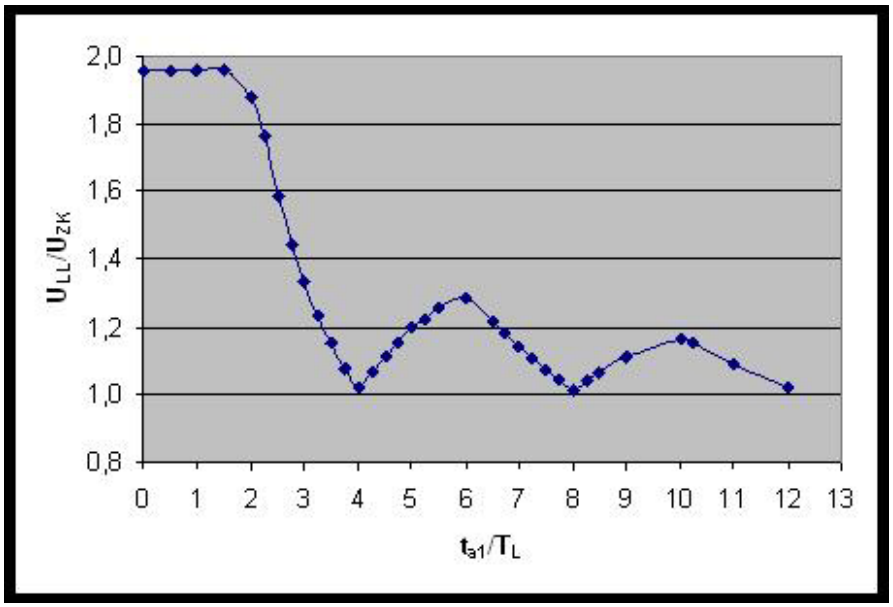

U_{LL}	phase-phase voltage at the machine
U_{ZK}	intermediate-circuit voltage at the inverter
t_{a1}	impulse rise time
T_L	duration time on the line

Fig 8.1: Over-voltage at the machine dependent on the length of line

For lines above a specified length, called "critical length", the voltage at the machine terminals reaches values of two times the inverter voltage, see Fig. 8.1. But the insulation of the machine

winding is designed for just 10 % … 20 % over-voltage. Therefore the insulation and finally the winding might be destroyed after a certain time in service.

8.2 Use of varistors to limit the over-voltages

In the given subproject the reduction of the aforementioned over-voltages with the help of metal-oxide (MO) varistor discs is investigated. Under these particular operating conditions the varistor is permanently stressed by over-voltage impulses. Therefore this is a new and non-conventional application for varistors, and the most severe problems are correct dimensioning and aging and lifetime issues, respectively.

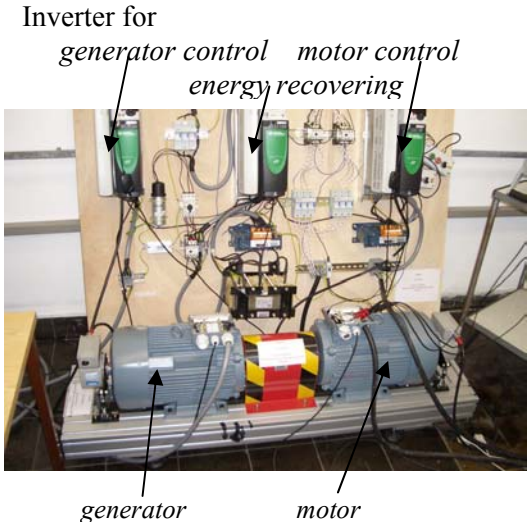

Fig. 8.2: Experimental set-up

In Fig. 8.2 the experimental set-up is shown. It consists of two machines, one used as motor and one as generator, and three inverters, one for motor speed control, one for generator torque control and one for energy recovering.

The first part of the project dealt with basic analysis of the set-up, which means detailed understanding of the interaction of the inverters and the machines, over-voltage phenomena etc. This was done in a diploma project of Mrs. Arefeh Danesh from January 2006 to June 2006.

The next focus was on the general varistor behaviour under the particular operating conditions. In Fig. 8.3 reduction of the over-voltage by a varistor can be recognized. The upper oscillogram of Fig. 3 shows the voltage at the machine without any over-voltage protection. While the intermediate-circuit voltage at the inverter is 600 V, the peak voltage at the machine is 1150 V (which is almost a doubling of the voltage). The second oscillogram of Fig. 3 shows the voltage at the machine when a varistor is connected in parallel to ground. In this case the voltage at the machine is reduced to 900 V. The current through the varistor is depicted in green color. Two high peeks are conspicuous. The first one is caused by the varistor capacitance, which is in the range of

$$C_{\mathrm{var}} = 12\,\mathrm{nF},$$

the second peek represents the resistive current where the resistance of the varistor is rather low and power is dissipated. At that time instant voltage and current are in phase. For the rest of the time the current is almost merely capacitive. Compared to the ordinary use of varistors under 50–

Hz alternating voltage stress, here the stress for the varistor is much higher due to pulse frequencies between 1 kHz … 20 kHz. The energy stress is permanently present, several thousand times per second, and there is no time for the varistor to relax thermally and electrically.

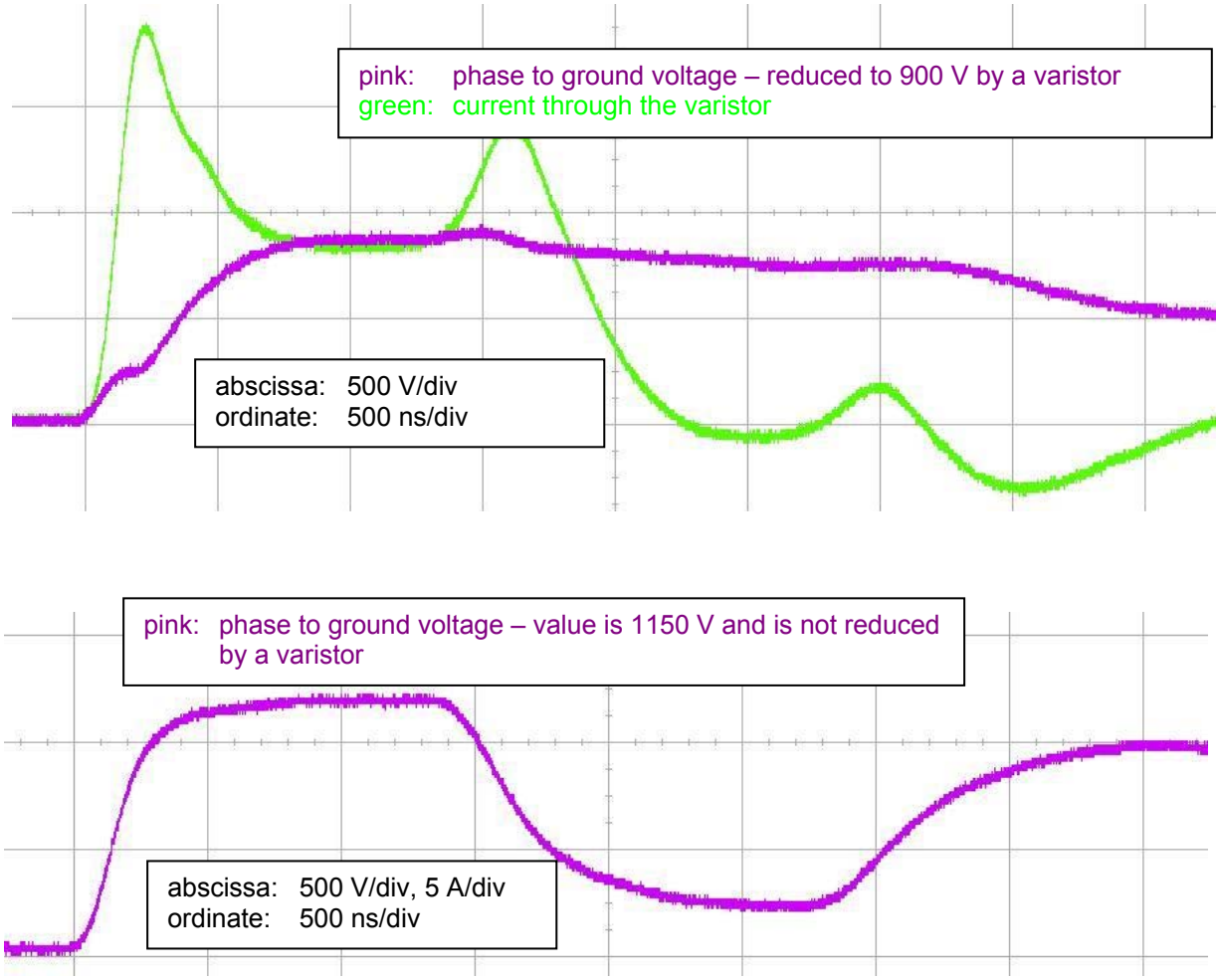

Fig. 8.3: top: Phase to ground voltage without varistor
bottom: Phase to ground voltage reduced by a varistor, current through the varistor

One final goal of the future work is the determination of a possible continuous operating voltage U_{ct} depending on pulse frequency, cable length, ambient temperature and temporary over-voltages.

Another important effect when using varistors in this application is the increase of rise time of the impulses caused by the large additional capacitance of the varistor disc, see Fig. 8.3. This is an additional positive effect with regard to the lifetime of the machine winding.

8.3 Ageing with impulse test voltage

Possible electrical aging during service is also a concern in this application. A setup for an accelerated aging test under impulse stress is actually under construction. An impulse test voltage source has been developed and implemented. It may be adjusted to amplitudes in the range of 0 V … 300 V and to frequencies between 4,5 kHz and 20 kHz. A connected cable of adequate length produces the typical over-voltages. Fig. 8.4 gives a typical example of the test voltage for the accelerated aging test procedure under investigation, and Fig. 8.5. shows a block diagram of the test set-up.

Under conventional (AC) conditions the accelerated aging test on varistors is performed at 1.05 times of its continuous operating voltage for a time duration of 1000 h and at a controlled varistor temperature of 115 °C. Successfully passing this test means that the power loss of the varistor permanently decreases; at least it should not increase. Details for evaluation are given in the standard *IEC 60099-4, ed. 2.1, clause 8.5.2*.

Normally, power losses of typical test samples are in the range of 300 mW … 2000 mW. But in this particular case of permanent high frequency impulse stress power loss is in the range of at least 15 W and more. Due to the risk of thermal runaway it is not possible to perform the test at a temperature of 115 °C and at constant voltage. It was therefore decided to alternatively control the power loss and keep it constant (e.g. to a value of 15 W) by varying the inverter voltage. In this case, criterion of a successful test is that the inverter voltage remains constant or increases with test time. It may decrease as well but should not fall below a specified value (e.g. 90% of the starting voltage). A similar aging test procedure (for varistors stressed above reference voltage) is specified in the standard *IEC 60099-4, ed. 2.1, 07/2006, clause 8.5.2.3*.

Passive cooling of the varistor discs is another important aspect of the current work. It is necessary to keep the temperature below a critical value to avoid thermal runaway. Also critical touch temperatures have to be considered. An appropriate varistor housing, including cooling elements, is therefore also under investigation.

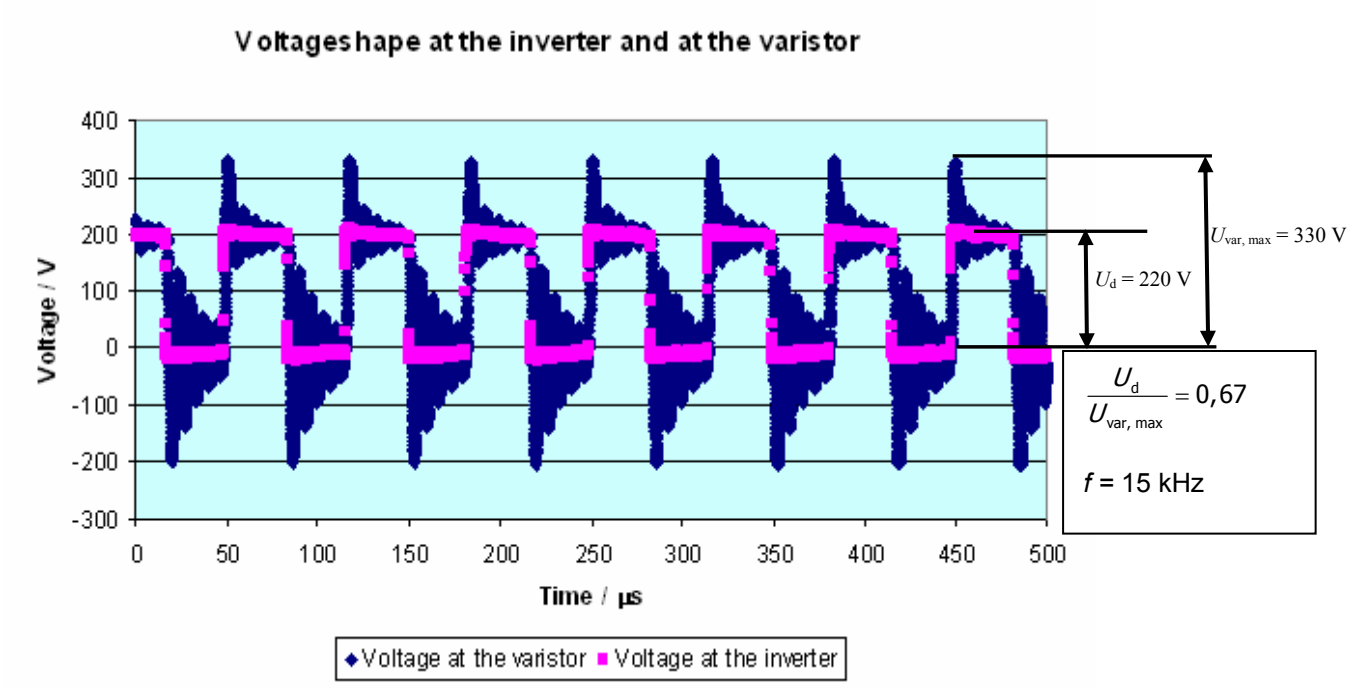

Fig 8.4: Shape of the test voltage

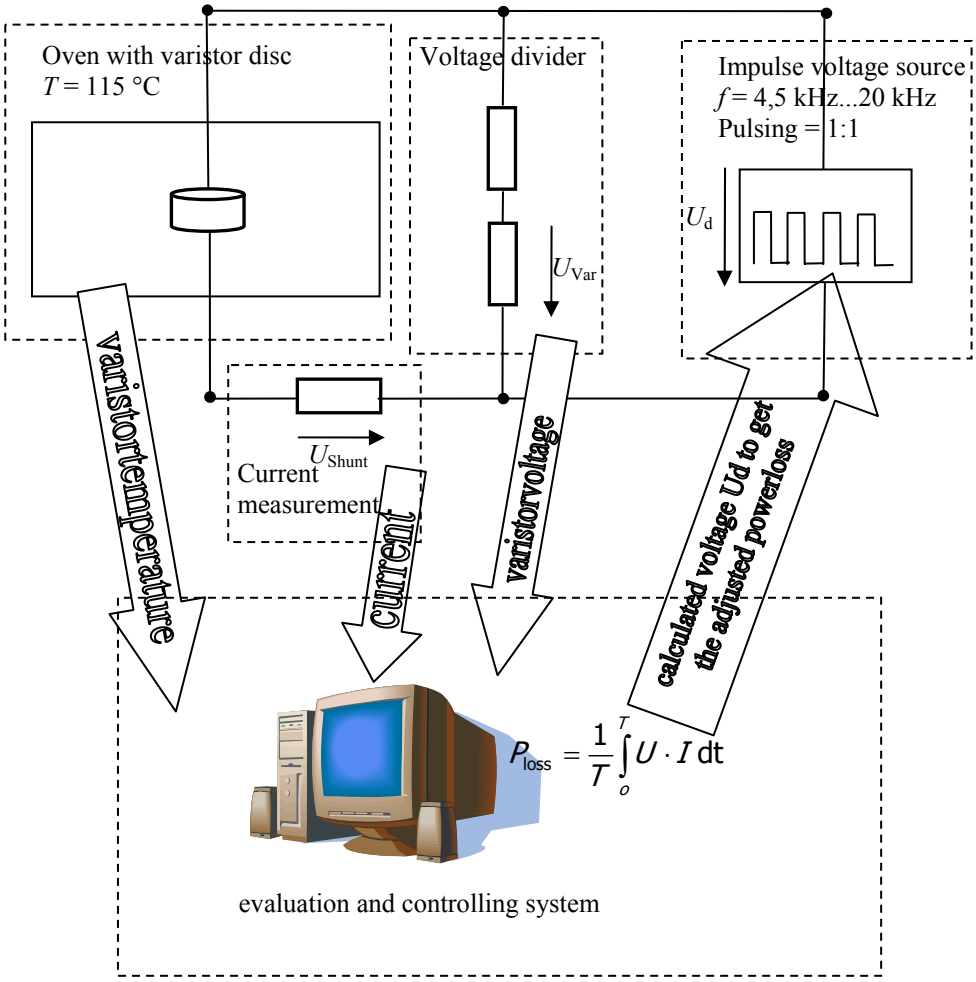

Fig. 8.5: Schematic depiction of the set-up

9. Subproject 5: Influencing the voltage slope at the inverter output by modifying the switching behaviour of the IGBT power modules, accomplished by special gate drivers

Prof. Dr.-Ing. Peter Mutschler
Dipl.-Ing. Calin Purcarea
Institut für Stromrichtertechnik und Antriebsregelung, TU Darmstadt
E-Mail: purcarea@srt.tu-darmstadt.de

9.1 Aim of the work

High frequency phenomena arises at fast switching elements, which deliver high voltage slopes at motor-terminals of 1kV/100ns. This can be achieved with fast switching IGBT (Field-stop Trench technology). The influences of voltage slope is to be observed and measured at motor terminals.
On the market exist 6-pack module inverters, including the control, DC-link circuit and the driver at very convenient prices (IPMs). But these IPMs cannot be used in this project, as the accessibility to measure intermediate quantities like collector current or collector-emitter voltage for a single IGBT is rather poor or inexistent. When measuring at output of the inverter module, the superposition of the parasitic module elements affect the measurement results. Also it is

necessary to measure the driver output quantities, which correspond directly to IGBT module and to modify the driver's characteristic.
Therefore, inverter and driving circuits have to be realized in this project in such a way that the necessary measurements are possible.

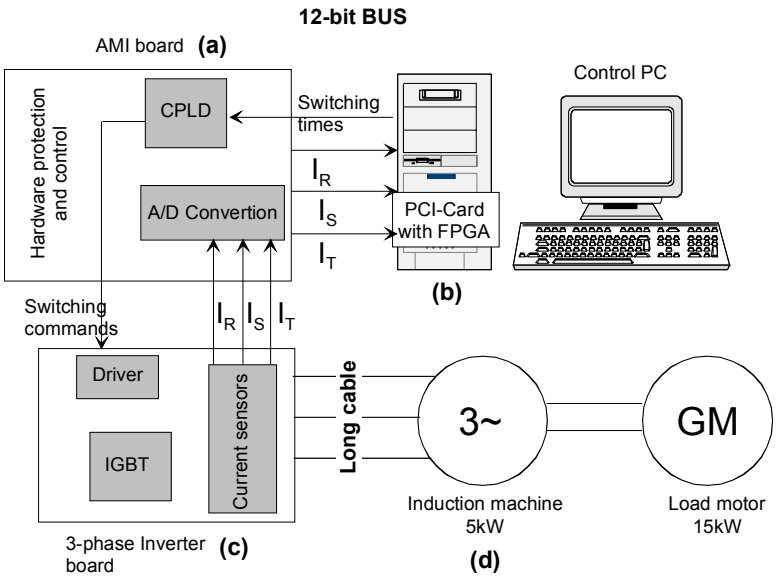

Fig. 9.1: Inverter-Cable-Motor system and control equipment

9.2 Need for building of a test-bench

Simulation models have to be developed to reflect the high-frequency behaviours of the inverter, cable and motor. These models have to correspond with state of the art of inverter-fed drive systems. Thus, switching behaviour of inverter elements with their disturbances through driver switching commands can be investigated, as well as parasitic capacities and inductances in the inverter's circuit.
In order to design suited models for inverter-cable-motor systems in time domain simulation, measurements on a real system must be conducted. Thus, the entire system including the inverter with the necessary control equipment, the cable and the motor must be built and the simulation results compared with the measurements on a real system.

9.3 Work done so far and achieved knowledge

The Inverter-Cable-Motor system was designed and constructed as shown in Fig. 9.1, where two main parts can be identified: power processing part and information processing part.

9.3.1. Information processing part

To control the inverter via the PC, an interface hardware called AMI (a) (Antriebs Module Interface) is used. This hardware provides the switching impulses for each transistor of the IGBT module and transforms the currents from analogue to digital values. The communication with the control PC is realized with a bus-system, where data transmission is synchronised to the switching of the inverter. Data receiving and sending over this bus is controlled by a CPLD. The switching commands are coming from the controller-PC and the acquired values for currents are sent back to the digital controller in the PC.

The CPLD realises also the interlocking time delay between switches of the upper and lower IGBT-arm in order to avoid short-circuit. Also on AMI-board, the over- current protection is realized in hardware.
The switching signals are generated by an interface board located in the control-PC and connecting to the PCI-bus of the PC. This board is called FZI (b). The control of FZI is made with FPGA and the communication with the computer is based on interrupts. The bus-system clock is acquired from PCI bus of the computer and sent via Bus to AMI board. Data receiving and sending is controlled using three control signals. Also on FZI, the galvanic isolation between the control hardware and the PC using optocouplers is implemented.
It should be mentioned that both AMI board and FZI board were developed at "Institut für Stromrichtertechnik und Antriebsregelung" within the framework of a previous project, and they were adapted for actual test bench.
The control itself consists of a C-code program running under DOS4GW, the real-time extension for DOS operating system or alternatively under RT-Linux. A simple Voltage-Frequency characteristic algorithm is used to control the armature voltage as a function of nominal voltage, nominal speed and instant value of speed.
In the C-code also the acquisition of instant values of inverter output currents is implemented.

9.3.2 Power processing part

On the Inverter Board (c) there are the 6-pack IGBT module, the driver, the DC-link capacitor, the bridge rectifier (for an optional supply directly from 3-phase grid) and the current sensors. Currently the DC-link is fed via an external high-voltage power supply, which is isolated by a three-phase transformer. On DC-link exists an interruption in order to connect the charging-protection resistor for capacitors. The DC-link is designed to be as near as possible to the IGBT module in order to avoid parasitic inductances, which generates oscillations in the DC-link voltage. The AMI board supplies the switching signals to the driver module, commutating further the gate of every IGBT of the 6-pack module. In gate of every IGBT there is the possibility to change the value of gate resistors R_{Gon} and R_{Goff}, thus changing the switching behaviour of the IGBT. Also on the Inverter Board the Current sensors are isolated from the power processing part. The current acquisition is further sent to AMI board where the measurements are digitised. From the inverter board the motor is fed by a cable. For the first measurements, only a short cable of 3m was used. For future measurements, longer cables will be used too. This cable has a 3-phase layout with screen. It must be specified that the minus bus of the DC-Link and the screen of the cable are both connected to earth. The motor (d) is an induction machine of 5 kW rated power and 17 A rated current. The rotor is a squirrel-cage type and mechanically coupled with a DC-machine of 15 kW rated power. At first only the induction machine is supplied with energy, thus having a no-load operation condition.

a) Measurement shunt resistor

The layout of 6-pack IGBT module allows measuring of collector current for a single IGBT by means of a shunt resistor connected between the emitter of BOT 3 and emitter of BOT 2. A coaxial shunt resistor, suited for high-frequency measurements, was designed and built to have a total resistance of 23 mΩ. This value allows a voltage drop across the shunt of 1.15V for a current of 50 A. Manganin composite (0.1mm layer thickness) was used for this shunt because of its small temperature-dependency coefficient ($\alpha = 0.01 \cdot 10^{-3}\,\mathrm{K}^{-1}$).

b) Commissioning of test-bench

Several test were made in order to prove the function and to check the limits according to data sheets:

- DC-Link voltage test up to 750V
- Continuous test current for inverter with 35 A
- Commissioning of Inverter module with a 5kW nominal power induction machine

- Proof of hardware monitoring and protection at exceeding nominal values for all three inverter-output currents.
- Proof of the communication between the AMI board and control PC via bus-system
- C-code program control proof under no-load machine operation

c) Conducted measurements

There were two types of measurements conducted to observe the difference between a stationary state of an inductive load and dynamic state with stator inductances of the motor.

9.4 Fixed load measurements

Following measurements are taken for only one phase of the machine, separated from the other two. It is used a "Buck-converter" configuration with lower IGBT from the third arm of module as switching element. The values measured for a single phase are: $L = 3$ mH, $R = 576$ mΩ.
Both turn-on and turn-off situations are plotted below.

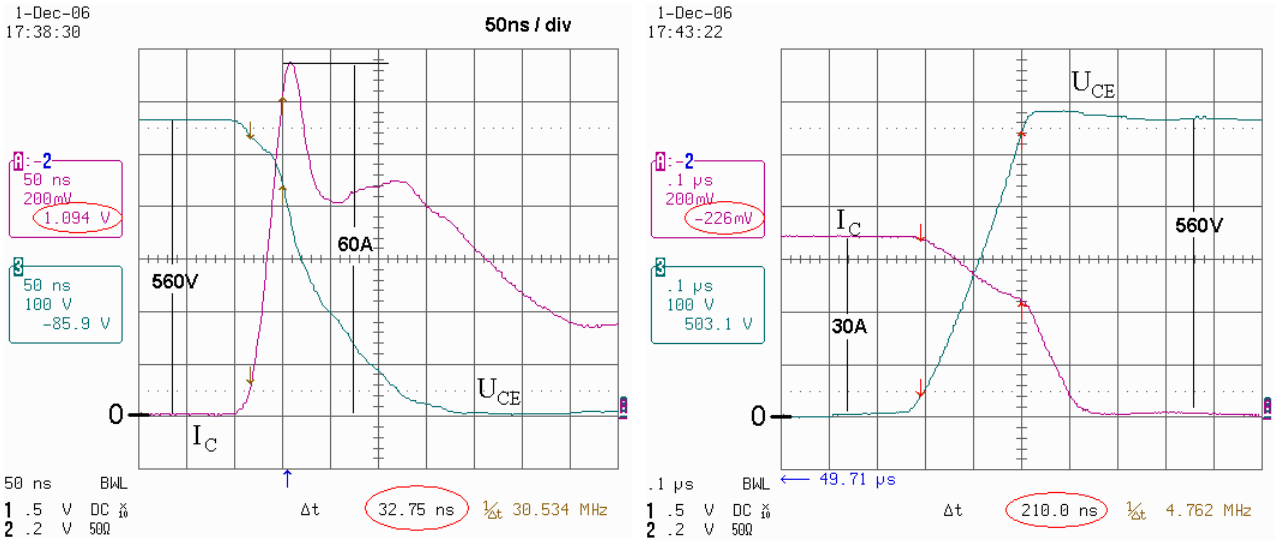

Fig. 9.2: Turn-on and turn-off behaviours by a single IGBT

It can be noticed the peak of reverse-recovery current. Marked with red the variation of current and time between $0{,}1I_{max}$ and $0{,}9I_{max}$ determines a slope of the current dI/dt of: $dI/dt = 48{,}26A/33{,}75ns \cong 1.44A/ns$. In Fig. 9.2 b) I_C and U_{CE} at IGBT's turn-off are shown. The collector-emitter voltage rises with the slope $dU/dt \cong 500V/200ns$. This slope is the main reason for over-voltages at motor terminals as shown later for full motor operation measurements. Also here can be noticed a decay of I_C as an effect of the parasitic capacity. The deviation measured and is marked with a red ellipse in Channel A data stream.

9.5 Motor operation measurements

The following conditions for the motor were considered: 560 V DC-Link voltage; 300 rpm speed of the machine; 3 m cable length between inverter and motor; no load for the induction machine. When the BOT3 IGBT turns-on (Figure 3b), the slope of U_{CE} (inverter-output voltage) produces stress on motor windings seen as oscillations in motor-terminal voltage, reflected also on collector current of IGBT. Considering the operation conditions this over-voltage has still a small value of 18%. At turning-off (Fig. 9.3b) the same effect of parasitic capacity can be observed. Thus, the current sinks before the collector-emitter voltage reaches a sufficient high value which allows the FWD to take the current from the inductive load. It is also noticed the appearance of voltage oscillation at the motor terminals when a fast dU/dt is applied, whereas the voltage at the output of

the inverter has practically no overshoot. The measurements show a voltage-slope of 500V/200ns. Till now the over-voltage is in reasonable limits because a short cable (3m) is used, but for the future the effect of different length of cables will be investigated

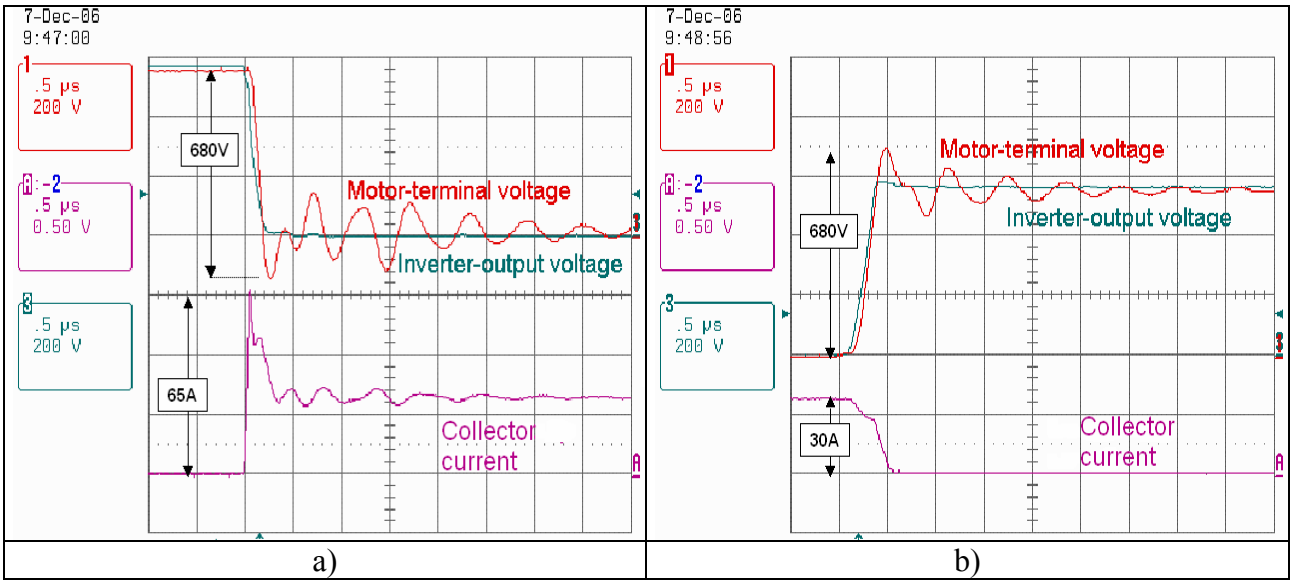

Fig. 9.3: Turn-on and turn-off of IGBT motor operation mode

9.6 Conclusions

The switching wave-forms for collector current I_C and collector-emitter voltage U_{CE} are similar with the ones given in literature. That demonstrates that the measuring system is correctly designed. The problem of the parasitic capacity must be further investigated and the measurements with other similar cases confronted.

9.7 References

[9.1] A. Wintrich "Verhaltungsmodellierung von Leistungshalbleitern für den rechnergestützten Entwurf leistugselektronischer Schaltungen", PhD thesis at TU-Chemnitz, Germany, 1996

[9.2] S. H. Stier, P. Mutschler "An Investigation of a reliable behavioral IGBT Model in comparison to PSpice and measurement in Hard- and Softswitching applications", European conference on Power Electronics and Applications, 2005

[9.3] P. Mutschler "Scriptum zur Vorlesung: Advance Power Electronics", TU-Darmstadt, 2002

10. Subproject 6: Multi-scale modelling and extraction of parameters in the simulation of inverter-fed drives

M.Sc. Zarife Çay
Prof. Dr. –Ing. Thomas Weiland
Institut für Theorie Elektromagnetischer Felder, TU Darmstadt
cay@temf.tu-darmstadt.de

10.1 Simulation of a Reluctance Machine

A 3D finite-element simulation of an exemplary reluctance machine (Fig. 10.1) is carried out by CST EM Studio [10] to obtain the torque in dependence of the rotor angle. Spurious torque components attributed to the angular resolution of the finite-element mesh are filtered out using

the FFT algorithm. A simple control scheme consists of applying a current to a coil whenever a positive contribution to the torque is expected. The equation of motion together with the angle-torque characteristic and the control strategy are integrated in time using a integrator for ordinary differential equations in Matlab.

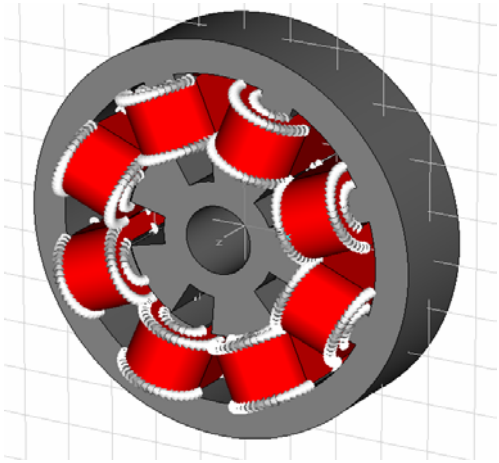

Fig. 10.1: Simulated reluctance machine.

10.2 Static Electro-Thermal Coupled Simulations using the Finite Integration Technique

In many electrical engineering applications, temperature effects cannot be neglected. Then, in the simulation, the electromagnetic field equation has to be accompanied by the thermal one. Difficulties in their numerical solution arise from the coupling between them and from the nonlinear nature of this coupling. A computational approach is developed to apply to such engineering problems. The algorithm is validated for a copper rod and a high-voltage varistor. The potential distribution at the steady-state (Fig. 10.2) indicates the higher resistivity due to the temperature increase in the middle of the rod.

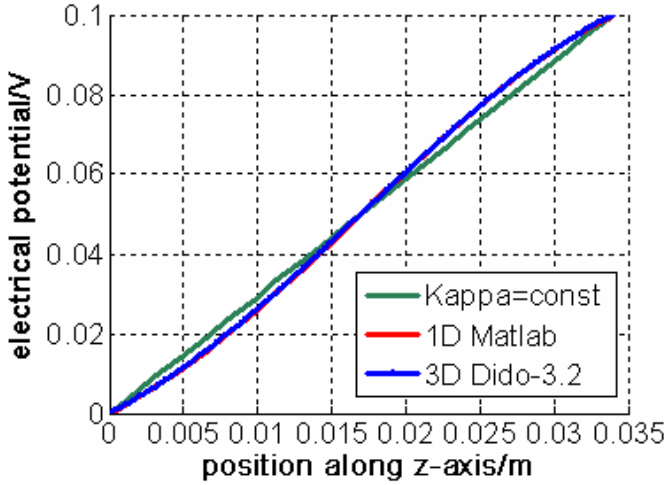

Fig. 10.2: Electrical potential variation of the copper rod model.

10.3 Transient Electro-quasi-static-Thermal Coupled Simulations using the Finite Integration Technique

We have focused on the design and implementation of iterative algorithms for the solution of

loosely coupled nonlinear transient electro-quasi-static-thermal problems. The thermal excitations in this study are electromagnetic losses due to pulsed voltage excitations. The partial differential equations describing the system are discretized in space using the finite integration technique (FIT). The spatial discretization results in ordinary differential equations that are further discretized in time by the theta method for the electro-quasi-static model and by an explicit scheme for the thermal model. The remaining nonlinearities are resolved by a Picard iteration.
The simulations of the copper rod and the ZnO varistor reflect the multi-physical behavior of these devices (Fig. 10.3). The time integration procedure reaches a steady-state situation, indicating that the explicit method applied to the thermal system is stable.

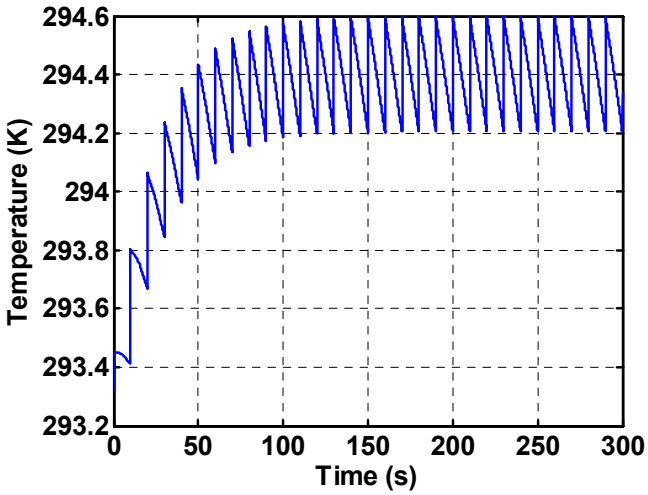

Fig. 10.3: Simulated temperature distribution monitored at the center point of the ZnO varistor excited by a pulse train with $V = 1.5967 \times 10^4$ V, $T_{pulse} = 2$ ms and $T_{period} = 1$ s.

10.4 2D Transient Electro-quasi-static Simulations

Several 2D Transient electro-quasi-static simulations of a distribution cable joint (Fig. 10.4) described in [10.8] are done for two different models (Fig. 10.5 and Fig. 10.6). The first model has linear material properties in every region whereas the second model has a nonlinear electrical conductivity in the mastic region.

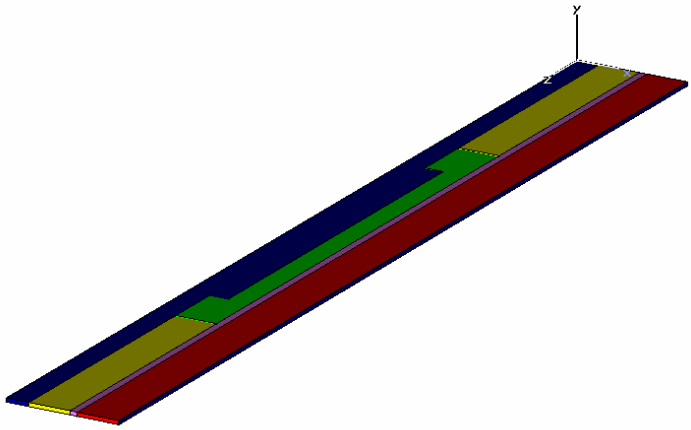

Fig. 10.4: 2D CST EM Studio [10.10] model of the distribution-cable-joint. The green region is the mastic region.

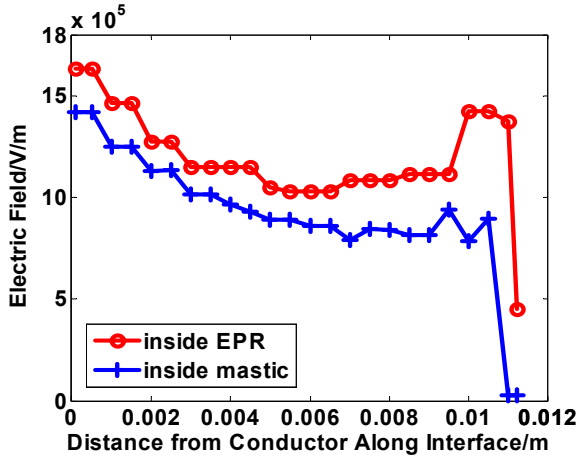

Fig. 10.5: Electrical field distribution of the linear distribution-cable-joint model excited by a sinusoidal voltage source

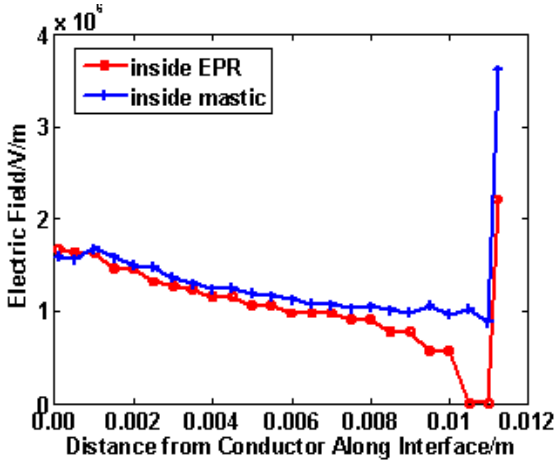

Fig. 10.6: Electrical field distribution of the nonlinear distribution-cable-joint model excited by a sinusoidal voltage source.

10.5 References

[10.1] M. Bartkowiak, M. G. Comber and G. D. Mahan, "Energy handling capability of ZnO varistors," *J. Appl. Phys.,* vol. 79, pp. 8629-8633, June 1996.

[10.2] S. Boggs, J. Kuang, H. Andoh and S. Nishiwaki, "Electro-thermal-mechanical computations in ZnO arrester elements," *IEEE Trans. Pow. Del.,* vol. 15, no. 1, pp.128-134, January 2000.

[10.3] J. Yuan, M. Clemens and T. Weiland, "Transient magnetic field calculations in hysteric media with FI²TD formulations," *Proceedings of Int. Conf. on Elec. Mach. Sys. ,* vol. 3, pp.769-773, November 2003.

[10.4] T. Weiland, "A discretization method for the solution of Maxwell`s equations for six-component fields," *Electronics and Communications AEÜ,* vol. 31, no. 3, pp.116-120, 1977.

[10.5] M. Clemens, E. Gjonaj, P. Pinder and T. Weiland, "Self-consistent simulations of transient heating effects in electrical devices using the finite integration technique," *IEEE Trans. Magn.,* vol. 37, no. 5, pp.3375-3379, September 2001.

[10.6] M. Schauer, P. Hammes, P. Thoma, T. Weiland, "Nonlinear update scheme for partially filled cells," *Proceedings of 10th Biennial IEEE Conf. EM Field Comp.,* Perugia, Italy, pp. 122, June 16-19, 2002.

[10.7] M. Clemens, M. Wilke, G. Benderskaya, H. De Gersem, W. Koch and T. Weiland, "Transient electro-quasistatic adaptive schemes," *Trans. Magn.*, vol. 40, no. 2, pp. 1294-1297, March 2004.

[10.8] J. B. Kuang and S. A. Boggs, "Application of Transient Nonlinear Field Analysis to a Distribution Cable Joint," *Annual Report of CEIDP*, 1995, p. 106-109.

[10.9] Z. Cay, H. De Gersem and T.Weiland, "Coupled Transient Electroquasistatic-Thermal Simulations using the Finite Integration Technique ," accepted for publication in COMPEL 3/2007.

[10.10] Computer Simulation Technology GmbH, www.cst.com